Broadband (600-1350 nm) Time Resolved Diffuse Optical Spectrometer for Clinical Use

Sanathana Konugolu Venkata Sekar, Alberto Dalla Mora, Ilaria Bargigia, Edoardo Martinenghi, Claus Lindner, Parisa Farzam, Marco Pagliazzi, Turgut Durduran, Paola Taroni, Antonio Pifferi, Andrea Farina

***Abstract*—We report on the design, development, and performance assessment of a portable time resolved system measuring absorption and scattering spectra of highly diffusive media over the 600-1350 nm range. In view of clinical use, two strategies were implemented; the first one equips the system with high responsivity in key tissue absorbing regions, whereas the second one makes the system immune to time drift. The MEDPHOT protocol was used for the performance assessment of the instrument. Finally, the system was enrolled into its first *in vivo* trial phase, measuring the broadband absorption and scattering spectra of human manubrium, abdomen fat tissues, and forehead for the *in vivo* quantification of key tissue constituents.**

***Index Terms*—Broadband, Time-Resolved, Turbid media, In-vivo, Silicon Photomultiplier (SiPM), Diffuse Optics, Absorption, Scattering.**

I. Introduction

DIFFUSE Optical Spectroscopy, in the past decade, has grown rapidly as a non-invasive optical tool to assess highly scattering media: *in-vivo* tissue characterization for the diagnosis of pathologies is a stunning example. More in detail, making best use of evolving technology, the field of photon migration in diffusive media branched out its application in numerous dimensions: optical mammography [1]–[4], *in vivo* tissue diagnosis[5][6], bone quality assessment [7][8], skin cancer diagnosis[9][10], brain monitoring [11][12], nondestructive assessment of food quality [13], wood characterization [14] and quality control of pharmaceutical tablets [15][16].

All these applications share the goal of measuring, possibly non-invasively, differential or absolute values of the optical properties – namely absorption (μ_a) and reduced scattering (μ_s') coefficients – over a broad spectral range in the near infrared (NIR region). The broadband estimation of μ_a and μ_s' yields information about chromophore concentrations and tissue structure, respectively [17].

Based on the configuration and type of source and detector, the study of photon migration in diffusive media can be classified mainly into: continuous wave (CW), frequency domain (FD) and time resolved (TR) techniques. CW techniques are based on the measurement of attenuation when light is injected and collected at different points of the sample [18]. In FD technique, the intensity of the injected light is sinusoidally modulated (typically at few frequencies) and the attenuation and phase shift of the detected signal is measured [19][20]. Time resolved techniques rely on the injection of a short light pulse (~ps) into the sample and on the temporal detection of the re-emitted light [21][22].

In literature, though there are no fully broadband FD systems, hybrid variants have been widely applied, where FD at a discrete set of wavelengths is used to find the regular shape of scattering spectra, and a space resolved CW measurement exploits these μ_s' values as prior information to estimate the μ_a spectrum [23]–[25]. In the last decade, taking advantage of new photonics devices and compact pulsed laser sources based on supercontinuum generation, time-resolved spectroscopy (TRS) systems have been strongly developed. Time resolved techniques have the unique capability to simultaneously estimate absorption and reduced scattering coefficients from a single measurement. This is due to the fact that, physically, μ_s'

The research leading to these results has partially received funding from LASERLAB-EUROPE (grant agreement n. 284464, EC's Seventh Framework Programme), OILTEBIA (grant agreement n. 317526), Fundació CELLEX Barcelona, l'Obra Social La Caixa MedLlumBCN). We acknowledge useful discussions with Mireia Mora and Mattia Squarcia.

Sanathana Konugolu Venkata Sekar, Alberto Dalla Mora, Edoardo Martinenghi, Paola Taroni, Antonio Pifferi are with Dipartimento di Fisica, Politecnico di Milano, Italy(e-mail: sanathana.konugolu@polimi.it;alberto.dallamora@polimi.it; edoardo.martinenghi@polimi.it;paola.taroni@polimi.it; antonio.pifferi@polimi.it).

Ilaria Bargigia is with Istituto Italiano di Tecnologia, Milan, Italy(email: Ilaria.Bargigia@iit.it).

Claus Lindner, Parisa Farzam, Marco Pagliazzi are with the ICFO-Institut de Ciències Fotòniques, The Barcelona Institute of Science and Technology, 08860 Castelldefels (Barcelona), Spain (e-mail: claus.lindner@icfo.es; pfarzam@mgh.harvard.edu;marco.pagliazzi@icfo.es).

Turgut Durduran is with ICFO-Institut de Ciències Fotòniques, The Barcelona Institute of Science and Technology, 08860 Castelldefels (Barcelona), Spain and Institució Catalana de Recerca i Estudis Avançats (ICREA), 08015 Barcelona, Spain. (e-mail: turgut,durduran@icfo.es).

Andrea Farina is with Consiglio Nazionale delle Ricerche - Istituto di Fotonica e Nanotecnologie, Piazza L. da Vinci 32, I-20133 Milano, Italy(e-mail: andrea.farina@polimi.it).

and μ_a affect differently the photon distribution at early and late detection times, respectively [22]. Moreover, operating in the time domain allows depth sectioning because the path length of the detected photons is directly encoded by the photon time-of-flight [26].

The first broadband time-domain system was implemented with a pulsed supercontinuum laser as broadband source and a parallel acquisition of the time resolved spectrum using a streak camera coupled to a spectrometer [27]. An improvement overcoming the low dynamic range and delicateness of the streak camera was achieved by using the time-correlated single-photon counting (TCSPC) technique [28], [29]. Along with high dynamic range and robustness, TCSPC provides sensitivity down to the single photon level. An evolution of TCSPC based broadband time resolved systems has been achieved using compact fiber laser sources based on supercontinuum generation [30] or diode lasers [1]. These systems, besides the reached compactness, cover only a part of the therapeutic window (600 nm-1100 nm).

In most of the in-vivo studies due to the limited number of available wavelengths (often selected in a restricted spectral range), oxy-, and deoxy-hemoglobin were assumed as the only absorbers in the tissue. Taking advantage of broadband spectroscopy, we can decouple the effect of additional absorbers in the tissue, which leads to more accurate estimation of tissue constituents. Major key tissue chromophores which are of interest to clinicians, namely lipid, water, and collagen, exhibit important absorption peaks, with significant high absorption in the 900-1300 nm range. However, the high tissue absorption in this range and the low detection efficiency of silicon based detectors beyond 1000 nm raise serious challenges on the side of system development.

Furthermore, carrying out *in vivo* studies in a clinical environment is quite challenging. Stability of the system, self-adaptation to quite diverse scenarios, automation and ease of use, along with portability and compactness are the prerequisites. Even a slight drift or distortion of the acquired curves, due to source and detector instability, can result in unwanted errors in the estimated measurable [31], [32]. Time resolved systems based on supercontinuum fiber lasers [30], though providing compactness, lag stability in the absence of a controlled laboratory environment.

In this paper, we show the development, validation and preliminary in-vivo test of a clinical TR system operating over a broad range of 600-1350 nm. Remarkably, a novel dedicated detection strategy addresses the issue of efficient light harvesting over so wide a range, whereas the real time acquisition of the Instrument Response Function (IRF) provides a self-stabilizing mechanism against unwanted drifts and distortions. Moreover, compactness, portability, and risk management are addressed in view of clinical applicability. The validation of the system is performed on tissue-simulating phantoms using the MEDPHOT Protocol which was agreed among several Institutions and is increasingly used for objective and quantitative performance assessment of diffuse optics instruments in retrieving optical properties of highly scattering media [33]. Finally, examples of *in vivo* application of the system for broadband spectral characterization of human tissues are presented, together with the retrieval of average tissue composition. To our knowledge, this is the first clinical system that permits non-invasive *in vivo* time-domain diffuse spectroscopy over so wide a spectral range.

II. System Design, Optimization and Data Analysis

A. Optical Chain

A schematic of the system's optical layout is shown in Fig. 1. To ensure patient safety and to facilitate compactness and applicability, we choose fibers for both delivery and collection of light pulses. A compact photonic crystal based pulsed supercontinuum fiber laser (SC450, Fianium, UK) driven at 40 MHz repetition rate is used as a broadband source.

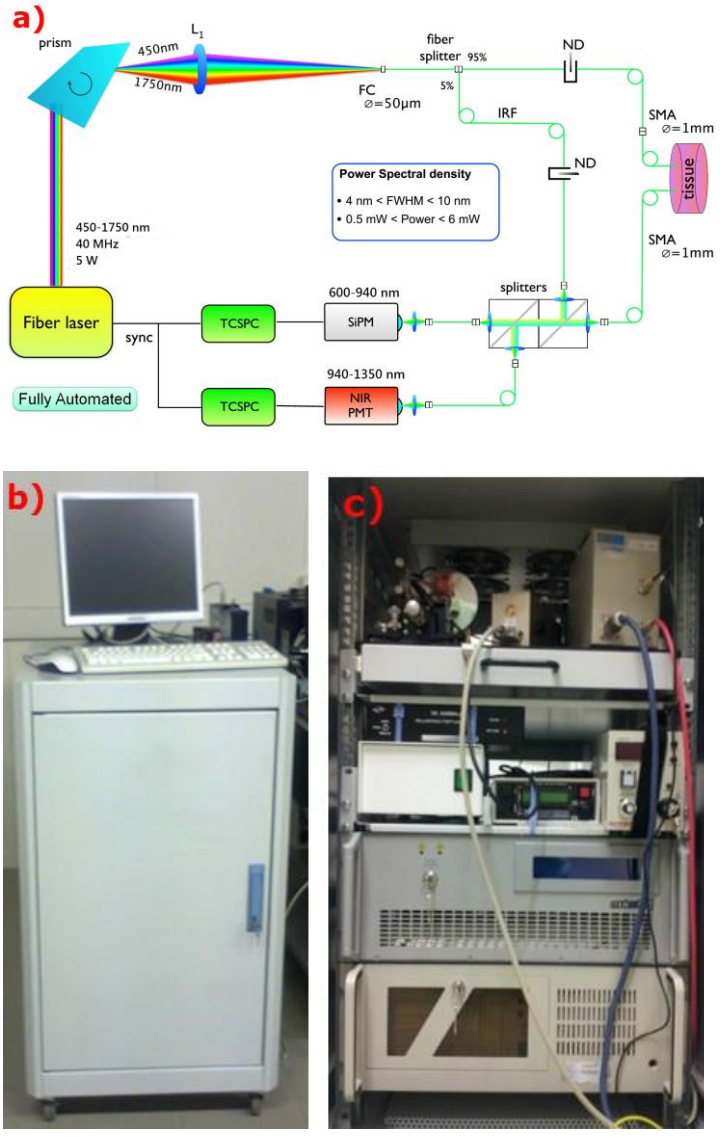

Fig. 1. (a) System's optical layout. The fiber network is represented by green lines. After the coupling of IRF with signal, two beam splitters distribute them to the detectors. (b) Picture of the portable system on wheels (111 x 81 x 61 cm). (c) Internal view of the system with optical chain arrangement on top and detector console, supercontinuum laser in the middle.

An F2 glass Pellin Broca prism disperses the supercontinuum light and a lens (f=150 mm) couples the minimum deviation wavelength into an optical fiber (core diameter of 50 µm). The wavelength tuning is achieved by the rotation of the prism. Due to the nonlinear dispersion of the prism, the spectral bandwidth ranges from 3 nm at 600 nm to 7 nm at 1350 nm. This selected light in turn is split into two parts 95% and 5%, the former acts as the source for sample measurement, while the latter as a reference arm for the simultaneous IRF acquisition to correct for drift and distortion. This strategy is elaborated in Subsection C. Tunable circular neutral density (ND) filters are used in both arms to adjust the power delivered, so as to avoid detector saturation. A multimode fiber of 1 mm-core is used as the collection fiber. The reference arm is combined back into the sample light arm with a suitable delay to share the same temporal window. A pellicle beam splitter in reverse configuration was chosen for this purpose. We avoided using dichroic or prism beam splitters, as our preliminary studies on them suggested that pellicle could minimize unwanted reflections and spectral distortions around the cut-off wavelength.

The uniqueness of the system is its high and almost flat responsivity (i.e. a figure of merit used in diffuse optics related to light harvesting [34]) over the entire working range of 600-1350 nm. To this purpose, we used two different detectors, namely a Silicon Photomultiplier (SiPM) (Hamamatsu S10362-11-050C) driven by a dedicated electronics developed at Politecnico di Milano [35] and an InGaAs photomultiplier (Hamamatsu mod.H10330A-45). To exploit their complementary spectral sensitivity (600-940 nm and 940-1350 nm, respectively), the signal is selectively directed onto the two detectors using a 45/55 pellicle beam-splitter with the spectral changeover point at 940 nm. Subsection B elucidates more on the selection of detectors. Signals from both detectors are fed into two TCSPC boards (SPC-130, Becker & Hickl, Germany), which acquire and store time resolved data.

B. Detection Strategies

The choice of the optimal detection strategy (i.e. combination of detectors and optical chain) was addressed exploiting the Basic Instrument Performances (BIP) Protocol [34] which identifies the key hardware features of a time-domain spectroscopy system. In particular, the following figures were considered: i) responsivity – assessed by considering the entire instrumentation including fibers, optics, attenuators and defined specifically for diffusion measurements, with distributed, quasi-Lambertian emission; ii) temporal shape of the IRF, and in particular its Full Width at Half Maximum (FWHM) and the decay tail; iii) Dark Count Rate (DCR). To quantify the responsivity, the BIP protocol prescribes to measure the signal detected through a calibrated solid phantom that simulates a diffusion environment. For the range 600nm to 850nm we used the tabulated calibration factor reported in Ref. [34], while for the other wavelengths we calculated the calibration factor analytically using the information on the μ_a and μ_s' of the phantom derived using a broadband laboratory workstation [36].

Five different time-resolved detectors, spanning a wide range of characteristics, were tested with this Protocol. For the lower Near Infrared (NIR) region (600-1000 nm) we considered a thick-junction Single-Photon Avalanche Diode (SPAD, 180 µm active area diameter, Excelitas Technologies), a thin-junction SPAD (100 µm active area diameter, MPD), two Silicon Photomultipliers (SiPM) by two different providers (1x1 mm^2 active area, Excelitas Technologies, and 1x1 mm^2, Hamamatsu) operated with custom dedicated electronics from Politecnico di Milano. For the upper NIR region (940-1350 nm) we tested an InGaAs Photomultiplier Tube (PMT, Hamamatsu). The desirable parameters are narrow IRF, low DCR, and high responsivity. Fig.2 shows the Responsivity (Fig. 2a) and IRF (Fig. 2b) of the detectors under study.

Though the thin-junction SPAD has very narrow IRF, comparable with SiPM, and the least DCR (Fig.2b), it lacks in responsivity by more than an order of magnitude as compared to other detectors (Fig. 2a). The reason of this behavior can be mainly the small (0.1 mm diameter) active area. On the contrary, the thick-junction detector has high responsivity (comparable to SiPM detectors), but its IRF suffers from a longer decay tail that can hamper the system performances [37]. Moreover, it has comparatively lower responsivity from 600 to 750 nm, where the absorption of hemoglobin is very high. Again, this is due to the relatively small area (0.18 mm diameter) of the detector, notwithstanding the higher photon detection efficiency of the thick-junction SPAD (e.g. >60% between 600 and 800 nm) as compared to the SiPM (~10% in the same range) in the whole spectral region considered in this study.

Due to lower responsivity, the selection of the thin-junction SPAD cannot be a good option; neither would be the thick-junction SPAD, as it suffers from long IRF tail along with comparatively low responsivity at key high absorbing regions of tissue. The two SiPMs have almost the same responsivity. From the inset table in Fig. 2(b), slightly narrower IRF and comparatively low DCR (60 kcounts per second, kcps) is observed in the case of Hamamatsu SiPM. Further, we found that Hamamatsu SiPM has slightly better linearity in retrieving μ_a and μ_s', compared to the other SiPM (data not shown). This led us to the conclusion of choosing the Hamamatsu SiPM for the lower NIR region. Finally, it is clearly seen from Fig. 2(b) that the Hamamatsu NIR PMT shows very high responsivity in upper NIR regions, forcing us to use this detector in the long wavelength range.

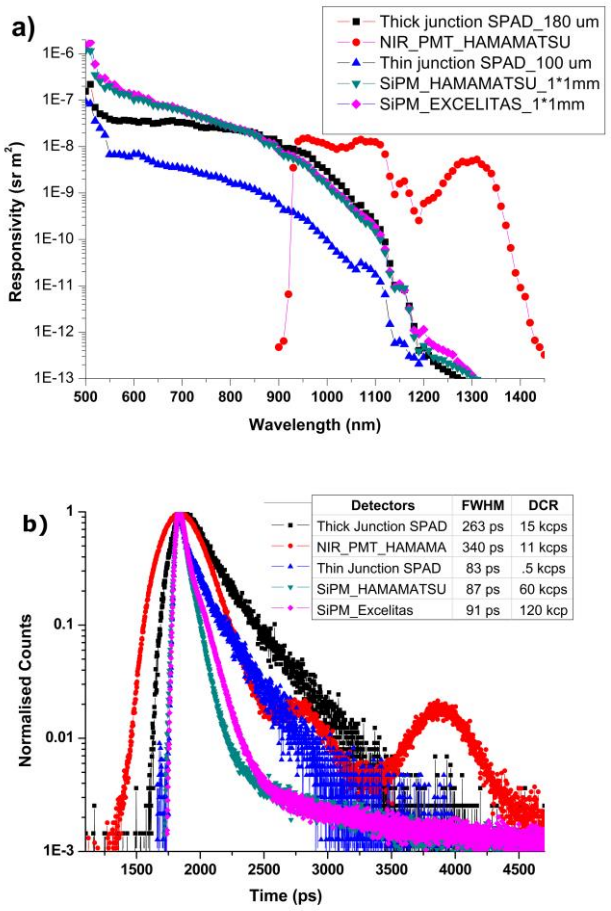

Fig. 2. (a) Broadband responsivity of detectors as function of wavelength: SiPM Hamamatsu and NIR_PMT show high responsivity in the lower and upper NIR regions respectively, and a good match at 940 nm. (b) IRF, with table inset showing the time jitter FWHM and DCR of detectors: narrowest IRF was observed for the thin junction SPAD and SiPM Hamamatsu.

The gradual reduction of SiPM responsivity at longer wavelengths, accompanied by the abrupt increase in PMT responsivity above 940 nm, suggests this wavelength as a good change over point. Interestingly, in this configuration, the lipid peak at 930 nm and 1040nm, the water peak around 980 nm followed by the collagen peak around 1030 nm will see high responsivity which enable good signal even with highly absorbing tissues. In summary, the system was implemented with SiPM (Hamamatsu) and InGaAs PMT (Hamamatsu) to cover efficiently the broadband range of 600-1350nm with changeover point at 940 nm.

C. *Drift and Distortion Compensation Strategy*

As it was elucidated in previous works [38], the stability of the IRF plays an important role in the overall stability and reproducibility of the system; even a slight drift or distortion in shape can directly affect the estimated μ_a and μ_s' values. This problem may get further amplified, if the system is moved from a controlled laboratory environment to an unpredictable clinical setting.

To make the system independent of possible drift and distortions caused by the clinical environment, we laid a reference arm to acquire the IRF along with the signal from the tissue: the last 2 ns of an 8 ns-window are devoted to the parallel acquisition of the IRF. This strategy is depicted in Fig. 3. Besides its use to account for possible time drifts, the reference can be exploited also as a substitute for the IRF used for fitting the data – after an initial calibration of the relative delay between the signal and the reference arms – thus resulting in a quicker operational procedure.

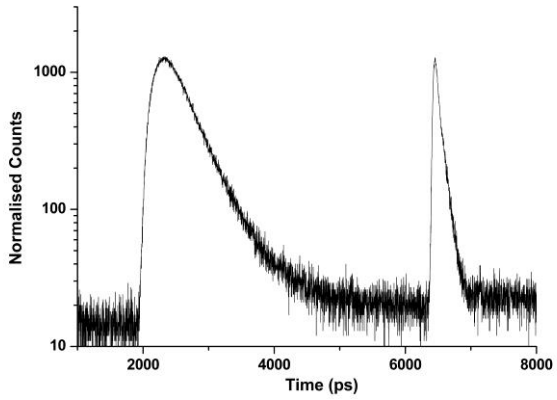

Fig. 3. Real time acquisition of the IRF, with diffused light signal in the beginning of the temporal window followed by a narrow IRF starting from 6000 ps.

D. *Measurement Operation and Timing*

An optimized proprietary software equips the system to analyze and display the μ_a and μ_s' data in real time. In exploratory studies, the wavelength tunability from any coarse to fine (5 nm) step size enables deeper understanding of narrow absorption peaks. The self-learning algorithm records the laser power attenuator tolerance of the *in vivo* location under study and optimizes the measurement time of 3 s per wavelength for first measurement to less 1 s per wavelength for consequent measurements. The system takes approximately a minute to acquire 76 wavelength over the broadband (600-1350 nm) range with 10 nm as step size, including the real time display of data and preserving the system performance at less than 3% coefficient of variation (CV). The entire process of wavelength tuning, power optimization, light collection, detector swapping at 940 nm, and data processing is completely automated.

E. *Data analysis*

TR temporal profiles are analyzed using analytical models based on the Diffusion Approximation to the Radiative Transport Equation with extrapolated boundary conditions [39]. The theoretical model is first convolved with the IRF (acquired by facing each other the injection and collection fibers), then the drift among the temporal barycenter of the reference curve and the one of the reference acquired with the IRF is calculated. According to this drift the theoretical model is temporally shifted. A nonlinear Levenberg-Marquardt optimization algorithm is finally applied for the estimation of μ_a and μ_s' that minimize the χ^2 merit function [40]. Signal lower than 80% of the peak on rising edge and lower than 1% on the falling edge is neglected. A dedicated online fitting tool is used to display the measured optical parameters in real time along with the acquisition. Thus, smooth visualization of the spectra

is available in real time during the measurements even for the shortest acquisition times compatible with an acceptable CV

III. Characterization And Performance Assessment

The MEDPHOT protocol [33], a well-established protocol in the time-resolved photon migration domain, defined and agreed by 21 European laboratories belonging to 8 different countries, was used for the characterization and performance assessment of our system. The protocol quantifies the instrument performances in retrieving the absorption and scattering properties of a diffusive homogeneous medium. Differently from BIP, the hardware performances are not tracked. Rather, the system is considered as a *black box* and only the final output in terms of retrieved μ_a and μ_s' are considered as measurands, over which the protocol is designed. More specifically, the MEDPHOT protocol assesses 5 figures, which are: a) accuracy in the retrieval of the absolute value of the optical properties, b) linearity in the relative tracking of optical changes, c) noise in the uncertainty of the retrieved optical coefficient, d) stability in the measured properties over short (minutes) and long (hours) time spans, e) reproducibility in measurements repeated identically in different days.

The protocol is implemented using a set of 32 solid phantoms made by a matrix of epoxy resin [41] with 4 concentrations of TiO_2 powder and 8 concentrations of black toner to vary μ_s' and μ_a in steps of about 5 cm^{-1} and 0.05 cm^{-1} respectively, spanning a wide range of μ_s' from 5 to 20 cm^{-1} and μ_a from 0 to 0.4 cm^{-1}.

In our study, we extracted a subset of 16 phantoms, combining in a matrix form 4 increasing absorption coefficients (0.05 to 0.35 cm^{-1}, respectively identified by numbers 2, 4, 6 and 8) with 4 increasing reduced scattering coefficients (5 to 20 cm^{-1}, respectively identified by letters A, B, C and D). All measurements were performed over the broad operating spectral range of 600-1350 nm with 10 nm as step size. Reflectance geometry with 2 cm as source-detector separation was used for the measurements.

Only for the first test (accuracy) we opted to use a liquid phantom, made of a water solution of Intralipid for two reasons. First, there is not yet acknowledged international consensus on the absolute characterization of the optical properties of the MEDPHOT solid phantom kit, with the last multi-laboratory exercise yielding still a 10-20% discrepancy among different laboratories [33]. Secondly, because water – the main absorber in a pure water solution of Intralipid, with no added ink – is well characterized spectrally and provides a straightforward way to span more than 2 decades in μ_a over the whole 600-1300 nm range, providing a highly challenging test.

A. Accuracy

Fig. 4. shows the absorption spectrum of a 1% (solid fraction) aqueous solution of Intralipid (blue squares) compared with the water spectra provided by D.J.Segelstein in the 600-710 nm range [42] (red line), by L. Kou et al. at 710-1100 nm [43] (black line), and Hale and Querry over entire broadband range 600-1350 nm [44] (green line). The water spectrum measured with our system is in good agreement with the published data and is generally comprised within the separation of the three reference spectra. There are significant discrepancies only for very low absorption ($\mu_a < 0.004$ cm^{-1}) – yet well below what normally expected in tissues – and for very high absorption ($\mu_a > 1$ cm^{-1}) because of lack of signal. There is also a clear difference around 1120 nm, which could be due to a bandwidth effect [45]. Indeed, the steepness of the water spectrum in that region combined with the increased bandwidth of the filtered supercontinuum (> 5 nm) can lead to a decreased fitted μ_a. However, it should also be taken into account that a limited number of data points is available from Ref. [44], leading to a coarse spectral sampling.

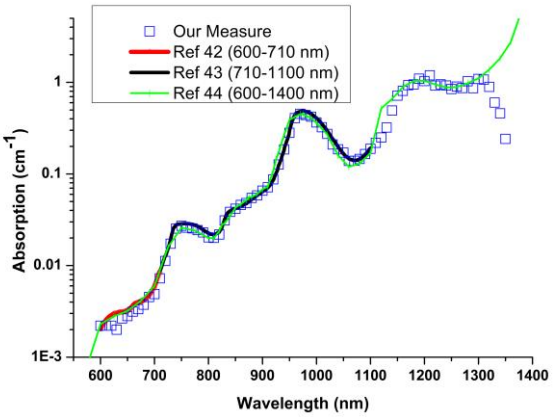

Fig. 4. Absorption spectrum of water as measured in a 1% aqueous solution of Intralipid using our system (blue squares) or reported in literature in Ref. 42 (red line), Ref. 43 (black line), and Ref. 44 (green line).

B. Linearity

Fig. 5 shows the results of the linearity test. This figure is divided into four sub diagrams: Fig. 5(a) and (d) plot the μ_a and μ_s' against their expected conventional true values, whereas Fig. 5(b) and (c) depict the coupling of μ_a and μ_s' with respect to each other. A solid line (linear fit) interpolates the plotted values. From Fig. 5(a), the interpolated curves of 4 different phantom series are almost overlapping, proving the independence of absorption estimates from scattering properties. Similar behavior is found for scattering which is shown in Fig. 5(d). Almost zero slope of fitted lines in Fig. 5(b) and (c) reconfirm the non-coupling nature of the system for a wide range of μ_s' and μ_a. Importantly, apart from the benefits of understanding the coupling and nonlinear behavior of the system, linearity plots can be used to compensate for wavelength specific coupling behavior between μ_a and μ_s'.

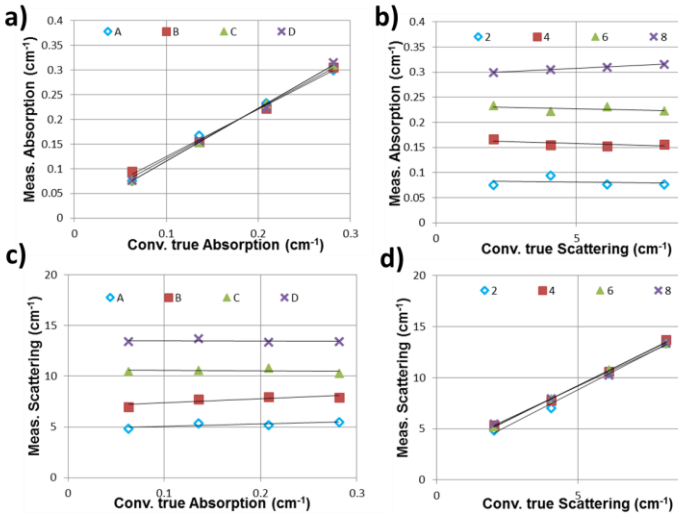

Fig. 5. Linearity assay of MEDPHOT protocol: measured absorption and scattering as a function of their conventional true values.

C. *Noise*

A set of 20 repeated measurements were performed on phantom B2 (nominal μ_a = 0.05 cm^{-1}, and μ_s' = 10 cm^{-1}) for 12 different photon count rates. Fig. 6 shows the coefficient of variation (CV) of the retrieved μ_s' and μ_a upon increasing the Total Counts. It is clearly seen that the total counts affect differently μ_s' and μ_a; for a given total counts μ_s' seems to have a relatively better CV than μ_a. The saturation in CV for μ_a at high total counts, suggests that a higher count rate is not going to improve drastically the system performance over a given signal threshold. Operating the system around 600 kcounts per second is the best condition to stay around 2% CV. When the system is operated at full single-photon counting statistics (i.e. whenever the signal is not dramatically low) this means that 1 s acquisition time per wavelength is sufficient.

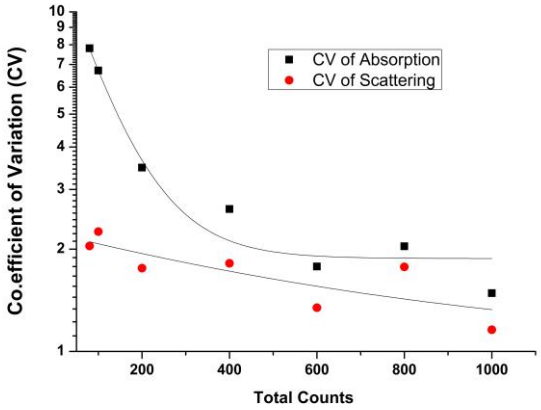

Fig. 6 Noise plots showing CV of absorption and reduced scattering as a function count rate (kcps).

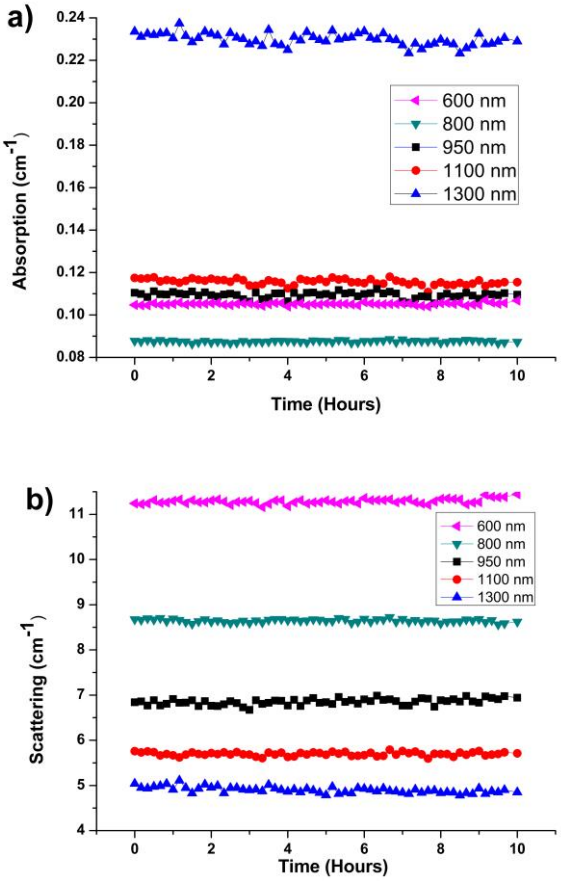

Fig. 7. Stability of the retrieved μ_a (a) and μ_s' (b) over 10 hours at different wavelengths.

D. *Stability*

Fig. 7(a),(b) display the stability of the system in retrieving μ_a and μ_s' for 10 hours of continuous measurements. Every 15 minutes the phantom B2 (same as above) was scanned over the entire broadband range (600 nm-1350 nm) at steps of 10 nm. There seems not to be major systematic drifts in the retrieved properties over the long-term measurements, while short-terms (<1 h) fluctuations are in the 3% range. It has to be observed that the stability would be strongly impaired if the reference stabilization were not performed.

E. *Reproducibility*

The reproducibility was calculated by measuring the same phantom B2 in the same reflectance geometry with 2 cm as source detector separation under the same experimental conditions on 60 different days. A CV lower than 4% (both for μ_s' and μ_a) at all wavelengths was observed.

IV. Preliminary *In vivo* Measurements

The developed system carried out its first successful *in vivo* trials on the human abdomen, manubrium, and forehead. The human subject's protocols were approved by the Hospital Clinic Barcelona ethical board. All subjects were informed about the study and associated risks and have signed a consent

form.

Measurements were performed in reflectance geometry with 2 cm source detector separation. Each *in vivo* measurement with pre-calibrated attenuator position took approximately 1 minute to acquire the 76 wavelengths of a broadband (600-1350 nm) spectrum. Fig. 8(a) shows the *in vivo* broadband absorption spectrum of the three locations. To estimate the concentration of various tissue constituents, the measured spectrum was fitted with the linear combination of tissue constituent spectra over the 600-1100 nm range (Beer law). The thick solid line in Fig. 8(a) shows the spectrum obtained by linear combination of tissue constituent spectra. Major tissue absorbers, namely water (H_2O), lipid, collagen, oxy and deoxy- hemoglobin (HbO_2 and Hb) and their corresponding absorption spectra were used for this purpose. A power law derived empirically from Mie theory, $\mu_s' = a(\lambda/\lambda_0)^{-b}$, with λ_0 = 600 nm, was used to fit the scattering spectrum in the range 600-850 nm. The corresponding values of the scattering amplitude (a) and power (b) are tabulated in Table 1.

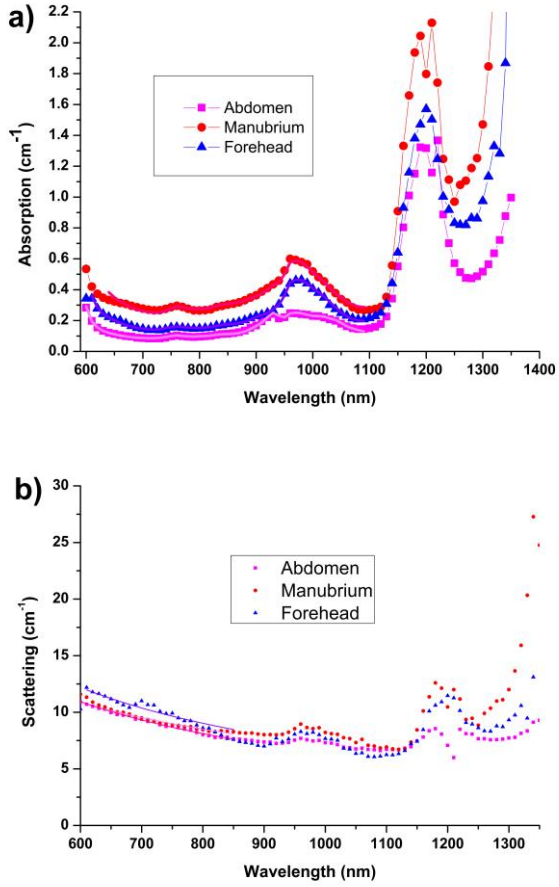

Fig. 8. (a) *In vivo* absorption (μ_a) and (b) reduced scattering (μ_s') spectra of human abdomen, manubrium and forehead. Thick solid lines show the linear combination fit of tissue absorption spectra in (a), and the fit to the empirical approximation of Mie theory in (b).

Table. 1. Tissue composition (concentration of lipids, water and collagen in mg/cm^3), blood parameters (tHb and SO_2), and scattering parameters (*a* and *b*).

In vivo Location	Hb (μM)	HbO_2 (μM)	tHb (μM)	SO_2 (%)	Lipid (mg/cm^3)	Water (mg/cm^3)	Collagen (mg/cm^3)	Bkg (cm^{-1})	a	b
Abdomen	3.2	13.9	17.1	81%	676	221	7	0.04	10.8	0.99
Manubrium	16.2	42.4	58.6	72%	329	552	17	0.13	10.9	0.84
Forehead	5.6	24.2	29.8	81%	174	590	43	0.04	13.0	1.41

Also the concentration of lipid, water, and collagen in mg/cm^3 and the micromolar concentration of Hb and HbO_2 are tabulated in Table 1, together with the total hemoglobin content tHb = HbO_2 + Hb and oxygen saturation level SO_2 = HbO_2/tHb. Manubrium, with a relatively superficial bone marrow tissue, exhibits high tHb concentration (58.6 μM) compared to other locations. The adipose nature of the abdomen is reflected with high lipid content (676 mg/cm^3). Signal from collagen, present in bone connecting tissue, due to skull, is seen evident (43 mg/cm^3) in the forehead region. Background (Bkg) in Table 1 is an estimation of possible missing components in our tissue spectra collection. SO_2, percentage oxygen saturation stays around 80%, with a minimum value of 72% in manubrium. The measured spectra were fitted only in the 600-1100 nm range since we lack complete spectral information on some of the main tissue absorbers beyond 1100 nm. Still there are interesting spectral features in the 1100-1300 nm range and we are working to consolidate reliable reference spectra for collagen and for Hb and HbO_2 in that long wavelength region. Possibly, other tissue constituents, with feeble spectral features at lower wavelengths could also play some major role in this extended region.

Decreasing scattering upon increasing wavelength is expected. As shown in Fig. 8(b), significant coupling between μ_a and μ_s' is observed at long wavelengths (above 1100 nm), where μ_a is high at all measurement locations. This effect is attributed to well-known limitations of the Diffusion theory in the interpretation of data collected in the present experimental conditions (high μ_a and comparatively low μ_s'), and was partially observed also in the linearity test, yet on a more limited range of μ_a. It is worth noting that this is independent of the instrumentation performance and better results could be obtained, for example, fitting to a library of Monte Carlo simulations [46]. Actually, the scattering spectrum can effectively be modeled with the simple power law (approximation to Mie theory). Thus, reliable information can be obtained even when the Diffusion model is applied, provided that a low-absorption subset of the entire spectral range is considered (*e.g.*, 600-900 nm) to fit the power law. Solid black lines in Fig. 8(b) show this empirical Mie theory fit to the measured μ_s'.

From Fig. 8(b), all measured *in vivo* locations seem to have roughly similar μ_s' values. Specifically, the forehead shows a higher scattering amplitude ($a \approx 13$, indicating higher density of scattering centers (*i.e.*, cellular interfaces and subcellular organelles), whereas the other two locations have similar values around 11). The forehead is also characterized by a higher scattering power *b*, as expected for scattering centers of smaller equivalent size ($b = 1.41$, while both other tissues have $b < 1$) [47].

Since the typical measurement time is around 1 minute for

the whole spectrum, it is possible to foresee a use of the system also to monitor dynamic changes *in vivo* in the time-scale of minutes/hours. Still, depending on the specific application, a dedicated characterization would be needed on the minimum measurement time required not to distort the reconstructed spectrum because of the transient optical values during the scan.

V. Conclusion

We developed and characterized the first system for diffuse optical spectroscopy that combines portability and suitability for clinical use with time domain operation (for accurate estimate of optical properties and, in turn, tissue composition and microscopic structure) with continuous spectral tuning over the unprecedented broad range of 600-1350 nm. First *in vivo* broadband time resolved measurements on the human abdomen, manubrium, and forehead are presented, revealing the spectral features of the key tissue constituents in this wide range and permitting to quantify their content. This instrument can be used in exploratory clinical studies aiming at full spectral characterization of either pathological or physiological conditions with an aim to noninvasive, optical diagnosis of disease. Translation to point-of-care, compact and cost effective portable devices is expected to become feasible in the next years due to the impressive growth of photonics components [48].

References

[1] R. Choe, S. D. Konecky, A. Corlu, K. Lee, T. Durduran, D. R. Busch, S. Pathak, B. J. Czerniecki, J. Tchou, D. L. Fraker, A. DeMichele, B. Chance, S. R. Arridge, M. Schweiger, J. P. Culver, M. D. Schnall, M. E. Putt, M. A. Rosen, and A. G. Yodh, "Differentiation of benign and malignant breast tumors by in-vivo three-dimensional parallel-plate diffuse optical tomography," *Journal of Biomedical Optics*, vol. 14. p. 024020, 2009.

[2] A. Pifferi, P. Taroni, A. Torricelli, F. Messina, R. Cubeddu, and G. Danesini, "Four-wavelength time-resolved optical mammography in the 680-980-nm range.," *Opt. Lett.*, vol. 28, no. 13, pp. 1138–40, Jul. 2003.

[3] A. Torricelli, L. Spinelli, A. Pifferi, P. Taroni, R. Cubeddu, and G. Danesini, "Use of a nonlinear perturbation approach for in vivo breast lesion characterization by multiwavelength time-resolved optical mammography.," *Opt. Express*, vol. 11, pp. 853–867, 2003.

[4] P. Taroni, A. Pifferi, E. Salvagnini, L. Spinelli, A. Torricelli, and R. Cubeddu, "Seven-wavelength time-resolved optical mammography extending beyond 1000 nm for breast collagen quantification," *Opt. Express*, vol. 17, no. 18, pp. 15932–15946, 2009.

[5] R. M. Doornbos, R. Lang, M. C. Aalders, F. W. Cross, and H. J. Sterenborg, "The determination of in vivo human tissue optical properties and absolute chromophore concentrations using spatially resolved steady-state diffuse reflectance spectroscopy.," *Phys. Med. Biol.*, vol. 44, pp. 967–981, 1999.

[6] P. Taroni, A. Pifferi, A. Torricelli, D. Cornelli, and R. Cubeddu, "In vivo absorption and scattering spectroscopy of biological tissues," *Photochem. Photobiol. Sci*, vol. 2, pp. 124–129, 2003.

[7] A. Pifferi, A. Torricelli, P. Taroni, A. Bassi, E. Chikoidze, E. Giambattistelli, and R. Cubeddu, "Optical biopsy of bone tissue: a step toward the diagnosis of bone pathologies.," *J. Biomed. Opt.*, vol. 9, no. 3, pp. 474–80, 2004.

[8] P. Farzam, P. Zirak, T. Binzoni, and T. Durduran, "Pulsatile and steady-state hemodynamics of the human patella bone by diffuse optical spectroscopy.," *Physiol. Meas.*, vol. 34, pp. 839–57, 2013.

[9] N. Rajaram, J. S. Reichenberg, M. R. Migden, T. H. Nguyen, and J. W. Tunnell, "Pilot clinical study for quantitative spectral diagnosis of non-melanoma skin cancer," *Lasers Surg. Med.*, vol. 42, pp. 716–727, 2010.

[10] S. F. Bish, M. Sharma, Y. Wang, N. J. Triesault, J. S. Reichenberg, J. X. J. Zhang, and J. W. Tunnell, "Handheld Diffuse Reflectance Spectral Imaging (DRSi) for in-vivo characterization of skin.," *Biomed. Opt. Express*, vol. 5, pp. 573–86, 2014.

[11] G. Bale, S. Mitra, J. Meek, and N. Robertson, "A new broadband near-infrared spectroscopy system for in-vivo measurements of cerebral cytochrome-c-oxidase changes in neonatal brain injury," vol. 36, no. 10, pp. 663–676, 2014.

[12] A. Torricelli, D. Contini, A. Pifferi, M. Caffini, R. Re, L. Zucchelli, and L. Spinelli, "Time domain functional NIRS imaging for human brain mapping," *Neuroimage*, vol. 85, pp. 28–50, 2014.

[13] R. Cubeddu, C. D'Andrea, A. Pifferi, P. Taroni, A. Torricelli, G. Valentini, C. Dover, D. Johnson, M. Ruiz-Altisent, and C. Valero, "Nondestructive quantification of chemical and physical properties of fruits by time-resolved reflectance spectroscopy in the wavelength range 650-1000 nm.," *Appl. Opt.*, vol. 40, pp. 538–543, 2001.

[14] A. Farina, I. Bargigia, E.-R. Janeček, Z. Walsh, C. D'Andrea, A. Nevin, M. Ramage, O. a Scherman, and A. Pifferi, "Nondestructive optical detection of monomer uptake in wood polymer composites.," *Opt. Lett.*, vol. 39, no. 2, pp. 228–231, Jan. 2014.

[15] Z. Sun, S. Torrance, F. K. McNeil-Watson, and E. M. Sevick-Muraca, "Application of frequency domain photon migration to particle size analysis and monitoring of pharmaceutical powders," *Anal. Chem.*, vol. 75, pp. 1720–1725, 2003.

[16] D. Khoptyar, A. A. Subash, S. Johansson, M. Saleem, A. Sparén, J. Johansson, and S. Andersson-Engels, "Broadband photon time-of-flight spectroscopy of pharmaceuticals and highly scattering plastics in the VIS and close NIR spectral ranges.," *Opt. Express*, vol. 21, pp. 20941–53, 2013.

[17] A. Pifferi, A. Farina, A. Torricelli, G. Quarto, R. Cubeddu, and P. Taroni, "Review: Time-domain broadband near infrared spectroscopy of the female breast: a focused review from basic principles to future perspectives," *J. Near Infrared Spectrosc.*, vol. 20, no. 1, pp. 223–235, 2012.

[18] S. Grabtchak and W. M. Whelan, "Separation of absorption and scattering properties of turbid media using relative spectrally resolved cw radiance measurements," *Biomed. Opt. Express*, vol. 3, no. 10, pp. 2059–2067, 2012.

[19] T. D. O'Sullivan, A. E. Cerussi, D. J. Cuccia, and B. J. Tromberg, "Diffuse optical imaging using spatially and temporally modulated light," *J. Biomed. Opt.*, vol. 17, p. 071311, 2012.

[20] B. W. Pogue and M. S. Patterson, "Frequency-domain optical absorption spectroscopy of finite tissue volumes using diffusion theory," *Phys. Med. Biol.*, vol. 39, no. 7, pp. 1157–1180, 1994.

[21] L. Dunne, J. Hebden, and I. Tachtsidis, "Oxygen Transport To Tissue XXIII," vol. 510, pp. 181–186, 2003.

[22] M. S. Patterson, B. Chance, and B. C. Wilson, "Time resolved reflectance and transmittance for the non- invasive measurement of tissue optical properties," *Appl. Opt.*, vol. 28, no. 12, pp. 2331–2336, 1989.

[23] F. Bevilacqua, A. J. Berger, A. E. Cerussi, D. Jakubowski, and B. J. Tromberg, "Broadband Absorption Spectroscopy in Turbid Media by Combined Frequency-Domain and Steady-State Methods," *Appl. Opt.*, vol. 39, no. 34, pp. 6498–6507, 2000.

[24] T. H. Pham, O. Coquoz, J. B. Fishkin, E. Anderson, and B. J. Tromberg, "Broad bandwidth frequency domain instrument for quantitative tissue optical spectroscopy," *Rev. Sci. Instrum.*, vol. 71, no. 6, p. 2500, 2000.

[25] J. P. Culver, R. Choe, M. J. Holboke, L. Zubkov, T. Durduran, A. Slemp, V. Ntziachristos, B. Chance, and A. G. Yodh, "Three-dimensional diffuse optical tomography in the parallel plane transmission geometry: evaluation of a hybrid frequency domain/continuous wave clinical system for breast imaging.," 2003.

[26] S. Del Bianco, F. Martelli, and G. Zaccanti, "Penetration depth of light re-emitted by a diffusive medium: theoretical and experimental investigation.," *Phys. Med. Biol.*, vol. 47, no. 23, pp. 4131–4144, Dec. 2002.

[27] C. af Klinteberg, A. Pifferi, S. Andersson-Engels, R. Cubeddu, and S. Svanberg, "In vivo absorption spectroscopy of tumor sensitizers with femtosecond white light.," *Appl. Opt.*, vol. 44, pp. 2213–2220, 2005.

[28] A. Pifferi, A. Torricelli, P. Taroni, D. Comelli, A. Bassi, and R. Cubeddu, "Fully automated time domain spectrometer for the absorption and scattering characterization of diffusive media," *Rev. Sci. Instrum.*, vol. 78, no. 5, p. 53103, 2007.

[29] A. Bassi, J. Swartling, C. D'Andrea, A. Pifferi, A. Torricelli, and R. Cubeddu, "Time-resolved spectrophotometer for turbid media based on supercontinuum generation in a photonic crystal fiber," *Opt. Lett.*, vol. 29, no. 20, pp. 2405–2407, 2004.

[30] A. Bassi, A. Farina, C. D'Andrea, A. Pifferi, G. Valentini, and R. Cubeddu, "Portable, large-bandwidth time-resolved system for diffuse optical spectroscopy.," *Opt. Express*, vol. 15, pp. 14482–14487, 2007.

[31] L. Spinelli, M. Botwicz, N. Zolek, M. Kacprzak, D. Milej, P. Sawosz, A. Liebert, U. Weigel, T. Durduran, F. Foschum, A. Kienle, F. Baribeau, S. Leclair, J.-P. Bouchard, I. Noiseux, P. Gallant, O. Mermut, A. Farina, A. Pifferi, A. Torricelli, R. Cubeddu, H.-C. Ho, M. Mazurenka, H. Wabnitz, K. Klauenberg, O. Bodnar, C. Elster, M. Bénazech-Lavoué, Y. Bérubé-Lauzière, F. Lesage, D. Khoptyar, A. A. Subash, S. Andersson-Engels, P. Di Ninni, F. Martelli, and G. Zaccanti, "Determination of reference values for optical properties of liquid phantoms based on Intralipid and India ink," *Biomed. Opt. Express*, vol. 5, no. 7, pp. 2037–2053, 2014.

[32] J. Bouchard, I. Veilleux, R. Jedidi, I. Noiseux, M. Fortin, and O. Mermut, "Reference optical phantoms for diffuse optical spectroscopy . Part 1 – Error analysis of a time resolved transmittance characterization method," *Opt. Express*, vol. 18, no. 11, pp. 1143–1155, 2010.

[33] A. Pifferi, A. Torricelli, A. Bassi, P. Taroni, R. Cubeddu, H. Wabnitz, D. Grosenick, M. Moller, R. Macdonald, J. Swartling, T. Svensson, S. Andersson-Engels, R. L. P. van Veen, H. J. C. M. Sterenborg, J. M. Tualle, H. L. Nghiem, S. Avriller, M. Whelan, and H. Stamm, "Performance assessment of photon migration instruments: the MEDPHOT protocol," *Appl. Opt.*, vol. 44, no. 11, pp. 2104–2114, 2005.

[34] H. Wabnitz, D. R. Taubert, M. Mazurenka, O. Steinkellner, A. Jelzow, R. Macdonald, D. Milej, P. Sawosz, M. Kacprzak, A. Liebert, R. Cooper, J. Hebden, A. Pifferi, A. Farina, I. Bargigia, D. Contini, M. Caffini, L. Zucchelli, L. Spinelli, R. Cubeddu, and A. Torricelli, "Performance assessment of time-domain optical brain imagers, part 1: basic instrumental performance protocol," *J. Biomed. Opt.*, vol. 19, no. 8, p. 86010, 2014.

[35] A. D. Mora, E. Martinenghi, D. Contini, A. Tosi, G. Boso, T. Durduran, S. Arridge, F. Martelli, A. Farina, A. Torricelli, and A. Pifferi, "Fast silicon photomultiplier improves signal harvesting and reduces complexity in time-domain diffuse optics," *Opt. Express*, vol. 23, no. 11, p. 13937, 2015.

[36] A. Pifferi, A. Torricelli, P. Taroni, D. Comelli, A. Bassi, and R. Cubeddu, "Fully automated time domain spectrometer for the absorption and scattering characterization of diffusive media," *Rev. Sci. Instrum.*, vol. 78, no. 5, p. –, 2007.

[37] D. Contini, A. Dalla Mora, L. Spinelli, A. Farina, A. Torricelli, R. Cubeddu, F. Martelli, G. Zaccanti, A. Tosi, G. Boso, F. Zappa, and A. Pifferi, "Effects of time-gated detection in diffuse optical imaging at short source-detector separation," *J. Phys. D. Appl. Phys.*, vol. 48, no. 4, p. 45401, 2015.

[38] R. Cubeddu, M. Musolino, A. Pifferi, P. Taroni, and G. Valentini, "Time-Resolved Reflectance: A Systematic Study for Application to the Optical Characterization of Tissues," *IEEE J. Quantum Electron.*, vol. 30, no. 10, pp. 2421–2430, 1994.

[39] D. Contini, F. Martelli, and G. Zaccanti, "Photon migration through a turbid slab described by a model based on diffusion approximation. I. Comparison with Monte Carlo results.," *Appl. Opt.*, vol. 36, no. 19, pp. 4587–4599, 1997.

[40] W. H. Press, S. A. Teukolsky, W. T. Vetterling, and B. P. Flannery, *Numerical Recipes: The Art of Scientific Computing*. Cambridge: Cambridge University Press, 1988.

[41] M. Firbank, M. Oda, and D. T. Delpy, "An improved design for a stable and reproducible phantom material for use in near-infrared spectroscopy and imaging.," *Phys. Med. Biol.*, vol. 40, pp. 955–961, 1995.

[42] D. Segelstein, "The complex refractive index of water," p. 167, 1981.

[43] L. Kou, D. Labrie, and P. Chylek, "Refractive indices of water and ice in the 0.65- to 2.5-μm spectral range.," *Appl. Opt.*, vol. 32, pp. 3531–3540, 1993.

[44] G. M. Hale and M. R. Querry, "Optical Constants of Water in the 200-nm to 200-μm Wavelength Region," *Applied Optics*, vol. 12. p. 555, 1973.

[45] A. Farina, I. Bargigia, P. Taroni, and A. Pifferi, "Note: Comparison between a prism-based and an acousto-optic tunable filter-based spectrometer for diffusive media," *Rev. Sci. Instrum.*, vol. 84, 2013.

[46] A. Pifferi, P. Taroni, G. Valentini, and S. Andersson-Engels, "Real-Time Method for Fitting Time-Resolved Reflectance and Transmittance Measurements with a Monte Carlo Model," *Appl. Opt.*, vol. 37, no. 13, p. 2774, May 1998.

[47] A. Farina, A. Torricelli, I. Bargigia, L. Spinelli, R. Cubeddu, F. Foschum, M. Jäger, E. Simon, O. Fugger, A. Kienle, F. Martelli, P. Di Ninni, G. Zaccanti, D. Milej, P. Sawosz, M. Kacprzak, A. Liebert, and A. Pifferi, "In-vivo multilaboratory investigation of theoptical properties of thehuman head," *Biomed. Opt. 2014*, vol. 6, no. 7, p. 238271, 2015.

[48] A. Dalla Mora, D. Contini, S. Arridge, F. Martelli, A. Tosi, G. Boso, A. Farina, T. Durduran, E. Martinenghi, A. Torricelli, and A. Pifferi, "Towards next-generation time-domain diffuse optics for extreme depth penetration and sensitivity," *Biomed. Opt. Express*, vol. 6, no. 5, pp. 1749–1760, 2015.

Sanathana Konugolu Venkata Sekar was born in Arani, Tamil Nadu, India, in March 1990. He received his Master degree in Physics (Gold Medalist) with Photonics specialization from Sri Sathya Sai Institute of Higher Learning, India, in 2013. Currently, he is pursuing his PhD at politecnico di Milano, Milan, Italy with Marie Curie ITN fellowship (acronym: OILTEBIA). His current area of research and interests are diffuse optical spectroscopy (DOS), DOS applied to *in vivo* clinical studies, Raman spectroscopy of diffusive media.

Alberto Dalla Mora was born in Fiorenzuola d'Arda, Italy, in 1981. He graduated summa cum laude in electronics engineering from the Politecnico di Milano, Italy, in 2006. He received the Ph.D. degree summa cum laude in information and communication technology from the same university in 2010. From 2010 to 2011 he was a Postdoctoral Fellow in the Dipartimento di Fisica of Politecnico di Milano, where since 2011 he has been Assistant Professor. Currently, his research interests include time-resolved diffuse spectroscopy instrumentations and applications for biomedical diagnosis.

Ilaria Bargigia was born in Milan on May 5, 1985. She received her Master degree in Physical Engineering from Politecnico di Milano, Italy, in 2009 and the PhD in Physics from the same University in 2013. Since January 2014 she has been a Postdoctoral Fellow in the Center for Nano Science and Technology @PoliMi - Istituto Italiano di Tecnologia, Milano, Italy. Her present research activity is mainly focused on time-resolved photoluminescence spectroscopy of light harvesting systems.

Edoardo Martinenghi was born in Milan, Italy, in September 1988. He graduated in electronics engineering from the Politecnico di Milano, Italy, in 2013. Currently, pursuing his PhD in the same University. His research interests are design of photodetectors for time domain diffuse optics and its application to biological media.

Claus Lindner was born in Göttingen, Germany, on April 8th, 1986. He received his Master of Science degree in Physics from the Ludwig-Maximilians-University, Germany, in 2011. Currently he's wokring on his PhD project in the Medical Optics group at the Institute of Photonic Sciences (ICFO). His current area of research is the use of near-infrared light to improve clinical screening and treatment methods in cancer and brain injury patients.

Parisa Farzam was born in Tehran, Iran, in 1983. She received her PhD in biomedical photonics from ICFO- The Institute of Photonics Sciences, Spain in 2014. Her research is focused on developing hybrid diffuse optics for monitoring of tissue hemodynamics. She is currently a research fellow at MGH, Harvard Medical School.

Marco Pagliazzi was born in Firenze, Italy, on 5th of April, 1987. He received his master degree in Physics from Università di Pisa, Italy, in 2012. Currently PhD student at ICFO, Barcelona, Spain. His current area of research is biomedical optics.

Turgut Durduran was trained at University of Pennsylvania (USA). In 2009, he has moved to ICFO-The Institute of Photonic Sciences (SPAIN) where he leads the "Medical Optics group". His research interests revolve around the use of diffuse light to non-invasively probe tissue function. The group develops new technologies and algorithms and translates them routinely to applications in pre-clinical and clinical as well for industries.

Paola Taroni was born in Como, Italy, in 1963. She received her degree in Nuclear Engineering from Politecnico di Milano, Milan, Italy, in 1987. Visiting scientist at M.I.T., Cambridge, MA, from 1987 to 1988. Staff researcher with the National Council for Research (CNR), Italy, Associate Professor of Physics at Politecnico di Milano from 1999 to 2010. Full Professor of Physics at Politecnico di Milano since 2011. Co-author of more than 120 scientific papers on internationally reviewed journals and 1 international patent. Her research activity concerns mainly the development of laser systems for time-resolved spectroscopy and imaging, and their applications in biology and medicine.

Antonio Pifferi was born in Milan in 1965. He graduated in Nuclear Engineering in 1991 and received his PhD in physics in 1995 at the Politecnico di Milano. Since 1996 he worked at the Physics Department of the Polytechnic of Milan, initially as a researcher and since 2003 as associate professor. His research focuses on the development and application of new laser techniques and instrumentation for diagnosis of pathologies. In particular, it is focused on the study of light propagation in highly scattering media with applications to optical characterization of biological tissues, optical mammography.

Andrea Farina was born in Milan on October 1, 1980. he received the Master degree (cum laude) in Electronics Engineering from Politecnico di Milano, Italy, in 2005 and the Ph.D. degree in Physics from Politecnico di Milano, Italy, in 2009. Since December 2011, he have a permanent position as researcher at the Institute of Photonics and Nanotechnologies (IFN) of the Italian National Research Council (CNR) in Milan. My current research includes the development and the application of new laser techniques for the spectral characterization of diffusive media using Time-Resolved Techniques.